A New Linear-Time Harmonic Balance Algorithm for Cyclostationary Noise Analysis in RF Circuits

J.S. Roychowdhury P. Feldmann

Bell Laboratories, Murray Hill, NJ

Abstract

A new technique is presented for computing noise in nonlinear circuits. The method is based on a formulation that uses *harmonic power spectral densities* (HPSDs), using which a block-structured matrix relation between the second-order statistics of noise within a circuit is derived. The HPSD formulation is used to devise a harmonic-balance-based noise algorithm that requires $O(nN \log N)$ time and $O(nN)$ memory, where n represents circuit size and N the number of harmonics of the large-signal steady state. The method treats device noise sources with arbitrarily shaped PSDs (including thermal, shot and flicker noises), handles noise input correlations and computes correlations between different outputs.

The HPSD formulation is also used to establish the non-intuituive result that *bandpass* filtering of cyclostationary noise can result in stationary noise.

The new technique is illustrated using an example that exhibits noise folding and interaction between harmonic PSD components. The results are validated against Monte-Carlo simulations. The noise performance of a large industrial integrated RF circuit (with >300 nodes) is also analyzed in less than 2 hours using the new method.

1 Introduction

In communication and signal-processing circuits, the random electrical noise that emanates from devices has a direct impact on critical higher-level specifications like SNR (signal to noise ratio) and BER (bit error rate). This makes it important to calculate circuit noise at the design stage. The complexity of most modern circuit designs makes computer-aided analysis the only practical means of predicting noise performance accurately.

Existing algorithms for noise computation in nonlinear circuits require computation and memory that scale quadratically or worse with the number of nonlinear devices. Until recently, this was not a limiting factor because traditional high-frequency communication circuitry used to be composed largely of linear elements and a few nonlinear devices. The present trend towards integration of RF circuitry is, however, reversing this paradigm. With IC techniques being applied to the design of on-chip RF circuitry, nonlinear devices are numerous and purely linear elements relatively few. Existing algorithms are impractically expensive for noise computation in such circuits.

Recently, efficient harmonic-balance algorithms for finding the steady state of large nonlinear circuits were proposed independently by Rösch and others [1, 2, 3] and Melville et al [4]. The algorithms achieve almost-linear performance by decomposing the harmonic balance jacobian matrix into simpler matrices that can be applied efficiently. This development alone does not, however, solve the problem of calculating nonlinear noise, because existing noise formulations cannot take advantage of the efficient harmonic balance decomposition. In this work, a new cyclostationary noise formulation is described that allows the efficient decomposition to be used, leading to the main contribution, an almost-linear algorithm for nonlinear noise.

The new formulation, an extension of the approach of Ström and Signell [5], uses *harmonic power spectral densities* (HPSDs) to represent the time-varying second-order statistics of cyclostationary noise. In Section 2, Ström and Signell's results are generalized to cyclostationary inputs and extended to obtain a block-structured matrix equation relating "output" noise statistics to "input" noise statistics. By exploiting circulant block structure, an efficient noise calculation procedure requiring $O(nN \log N)$ computation and $O(nN)$ memory is obtained (n is the circuit size, N the number of significant harmonics in its steady state).

Using the new algorithm, it is possible to compute the total noise at a specific output, correlations between noise at different outputs, as well as individual contributions from each noise generator to a specific output. Moreover, the noise formulation is capable of taking into account noise generators with any PSD shape (e.g., modulated shot, thermal and flicker noises) and can also handle correlated generators efficiently.

In a separate application of the HPSD formulation, it is proved (Section 3) that one-sided (or single-sideband) filtering of cyclostationary noise removes cyclostationary components to leave stationary noise. This non-intuitive result is confirmed in Section 4 by simulation with the new algorithm and also through extensive Monte-Carlo simulations. The usefulness of the algorithm for practical circuits is demonstrated by analyzing a large integrated-RF circuit, consisting of in-phase and quadrature filters and mixers, with about 360 nodes. The new algorithm calculates noise in this circuit in less than two hours using 50MB of memory.

0-7803-3662-3/97/$5.00©1997IEEE

2 Efficient cyclostationary noise computation algorithm

The equations of any nonlinear circuit can be expressed in the form:

$$\dot{q}(x(t)) + f(x(t)) + b(t) + Au(t) = 0 \qquad (1)$$

$x(t)$ are the time-domain circuit variables or unknowns, $b(t)$ is a vector of large-signal excitations, f and q represent the "resistive" and "dynamic" elements of the circuit respectively. The last term $Au(t)$ represents "small" perturbations to the system, e.g., from noise sources in devices. All these quantities are vectors of dimension n. $u(t)$ has dimension m, representing the number of noise sources in the circuit. A is an incidence matrix of size $n \times m$ which describes how these noise sources are connnected to the circuit.

Since the noise sources $u(t)$ are small, their effects can be analyzed by perturbing the noise-free solution of the circuit. Let $x^*(t)$ represent the large signal solution of Equation 1 with $u(t)$ set to zero. Performing a time-varying linearization of Equation 1 about x^*, the following linearized small-signal differential equation is obtained:

$$C(t)\,\dot{x} + G(t)\,x + A\,u(t) = 0 \qquad (2)$$

$x(t)$ in Equation 2 now represents the small-signal deviations of the perturbed solution of Equation 1 from the noise-free solution x^*. $C(t)$ and $G(t)$ are the derivative matrices of $f(\cdot)$ and $q(\cdot)$.

Equation 2 is a linear differential equation with time-varying coefficients. It therefore describes a linear time-varying (LTV) system with input $u(t)$ and output $x(t)$. The LTV system is characterized completely by its time-varying impulse response (or kernel) $h(t_2, t_1)$, a $n \times m$ matrix. The dependence of h on $C(t)$, $G(t)$ and A will be examined in Section 2.2; the propagation of noise through LTV systems is analyzed next.

2.1 Propagation of noise through a linear time-varying (LTV) system

The input-output relation of the LTV system described by Equation 2 is:

$$x(t_2) = \int_{-\infty}^{\infty} h(t_2, t_1) u(t_1)\, dt_1 \qquad (3)$$

The objective of this section is to obtain a relation between the statistics of u and x if they are stochastic processes. Assuming that they are nonstationary processes, their covariance matrices are defined as [6, 7, 5]:

$$R_{pp}(t_1, t_2) = E\left[p(t_1) p^T(t_2)\right] \qquad (4)$$

where p is u or x. A straightforward analysis establishes the following relation between R_{xx} and R_{uu}:

$$R_{xx}(t_1, t_2) = \int_{-\infty}^{\infty}\int_{-\infty}^{\infty} h(t_1, \tau_1)\, R_{uu}(\tau_1, \tau_2)\, h^T(t_2, \tau_2)\, d\tau_1\, d\tau_2 \qquad (5)$$

Most nonlinear systems of practical interest involve periodic waveforms. If $x^*(t)$, the unperturbed solution of Equation 1, is periodic with period T, then $C(t)$ and $G(t)$ of Equation 2 are also T-periodic. Hence $h(t_2, t_1)$ describes a linear *periodic* time-varying (LPTV) system, and $h(t_2, t_1)$ is periodic with respect to displacements of T in both its arguments, i.e.,

$$h(t_2 + T, t_1 + T) = h(t_2, t_1) \qquad (6)$$

The periodicity of h implies that it can be expanded in a Fourier series:

$$h(t_2, t_1) = \sum_{i=-\infty}^{\infty} h_i(t_2 - t_1)\, e^{ji\omega_0 t_2}, \qquad \omega_0 = \frac{2\pi}{T} \qquad (7)$$

h_i in the above equation are functions of one variable, and will be referred to as the *harmonic impulse responses* of the LPTV system. Moreover, their Fourier transforms will be denoted by H_i and referred to as the *harmonic transfer functions* of the LPTV system, i.e.,

$$H_i(\omega) = \int_{-\infty}^{\infty} h_i(t)\, e^{-j\omega t}\, dt \qquad (8)$$

Next, two-dimensional power spectral densities are defined by taking two-dimensional Fourier transforms of R_{xx} and R_{uu} [6, 5]:

$$S_{pp}(\omega_1, \omega_2) = \int_{-\infty}^{\infty}\int_{-\infty}^{\infty} R_{pp}(t_1, t_2)\, e^{-j\omega_1 t_1}\, e^{-j\omega_2 t_2}\, dt_1\, dt_2 \qquad (9)$$

By Fourier transforming Equation 5 and using the definitions in Equations 8-9, an expression relating S_{xx} and S_{uu} is obtained:

$$S_{xx}(\omega_1, \omega_2) = \sum_{i,k=-\infty}^{\infty} H_k(\omega_1 - k\omega_0)\, S_{uu}(\omega_1 - k\omega_0, \omega_2 - i\omega_0)\, H_i^T(\omega_2 - i\omega_0) \qquad (10)$$

The assumption that both input and output noises are *cyclostationary* is now introduced. The cyclostationary assumption implies that R_{xx} and R_{uu} do not change if T is added to both arguments, i.e.,

$$R_{pp}(t_1 + T, t_2 + T) = R_{pp}(t_1, t_2) \qquad (11)$$

Hence both can be expressed as Fourier series:

$$R_{pp}(t_1, t_2) = \sum_{i=-\infty}^{\infty} R_{pp_i}(t_2 - t_1)\, e^{ji\omega_0 t_2} \qquad (12)$$

R_{xx_i} and R_{uu_i} are functions of one variable and will be referred to as the *harmonic covariances* of the output and input noise respectively. Their (one-dimensional) Fourier transforms will be denoted by S_{xx_i} and S_{uu_i} and referred to as *harmonic PSDs* or *HPSDs*, i.e.,

$$S_{pp_i}(\omega) = \int_{-\infty}^{\infty} R_{pp_i}(t)\, e^{-j\omega t}\, dt \qquad (13)$$

The harmonic covariances and PSDs have simple physical interpretations. $R_{xx}(t,t)$ represents the time-varying power of the cyclostationary noise; hence by Equation 13, $R_{xx_i}(0)$ (the harmonic covariances evaluated at 0) represent the Fourier components of the periodically varying noise power. In particular, $R_{xx_0}(0)$ is the average value, or stationary component, of the power. From the definition of the harmonic PSDs, it follows that the harmonic covariances evaluated at 0 are equal to the corresponding harmonic PSDs integrated over the entire frequency axis. Hence $S_{xx_0}(\omega)$ integrated equals the stationary component of the output noise power. S_{xx_0} and S_{uu_0} will be therefore be termed *stationary PSDs.*

ary noise inputs of a similar equation by Ström and Signell [5]. An interesting and useful observation about Equation 15 is that the output harmonic l appears only in the last term $H^T_{l-(j+k)}$. This suggests that Equation 15 can be written in block matrix form. It can be verified by direct multiplication that Equation 15 is equivalent to the following block matrix equation:

$$\mathcal{S}_{xx}(\omega) = \mathcal{H}(\omega)\,\mathcal{S}_{uu}(\omega)\,\mathcal{H}^*(\omega) \tag{16}$$

where $\mathcal{H}^*$ denotes the Hermitian of $\mathcal{H}$. $\mathcal{S}_{xx}$, $\mathcal{S}_{uu}$ and $\mathcal{H}$ are block matrices with an infinite number of blocks, given by (denoting $w + k\omega_0$ by w^k for conciseness):

$$\mathcal{H}(\omega) = \begin{bmatrix} \vdots & \vdots & \vdots & \vdots & \vdots & \\ \cdots & H_0(\omega^2) & H_1(\omega^1) & H_2(\omega^0) & H_3(\omega^{-1}) & H_4(\omega^{-2}) & \cdots \\ \cdots & H_{-1}(\omega^2) & H_0(\omega^1) & H_1(\omega^0) & H_2(\omega^{-1}) & H_3(\omega^{-2}) & \cdots \\ \cdots & H_{-2}(\omega^2) & H_{-1}(\omega^1) & H_0(\omega^0) & H_1(\omega^{-1}) & H_2(\omega^{-2}) & \cdots \\ \cdots & H_{-3}(\omega^2) & H_{-2}(\omega^1) & H_{-1}(\omega^0) & H_0(\omega^{-1}) & H_1(\omega^{-2}) & \cdots \\ \cdots & H_{-4}(\omega^2) & H_{-3}(\omega^1) & H_{-2}(\omega^0) & H_{-1}(\omega^{-1}) & H_0(\omega^{-2}) & \cdots \\ & \vdots & \vdots & \vdots & \vdots & \vdots & \end{bmatrix} \tag{17}$$

$$\mathcal{S}_{xx}(\omega) = \begin{bmatrix} \vdots & \vdots & \vdots & \vdots & \vdots & \\ \cdots & S_{xx_0}(-\omega^2) & S_{xx_1}(-\omega^2) & S_{xx_2}(-\omega^2) & S_{xx_3}(-\omega^2) & S_{xx_4}(-\omega^2) & \cdots \\ \cdots & S_{xx_{-1}}(-\omega^1) & S_{xx_0}(-\omega^1) & S_{xx_1}(-\omega^1) & S_{xx_2}(-\omega^1) & S_{xx_3}(-\omega^2) & \cdots \\ \cdots & S_{xx_{-2}}(-\omega^0) & S_{xx_{-1}}(-\omega^0) & S_{xx_0}(-\omega^0) & S_{xx_1}(-\omega^0) & S_{xx_2}(-\omega^0) & \cdots \\ \cdots & S_{xx_{-3}}(-\omega^{-1}) & S_{xx_{-2}}(-\omega^{-1}) & S_{xx_{-1}}(-\omega^{-1}) & S_{xx_0}(-\omega^{-1}) & S_{xx_1}(-\omega^{-1}) & \cdots \\ \cdots & S_{xx_{-4}}(-\omega^{-2}) & S_{xx_{-3}}(-\omega^{-2}) & S_{xx_{-2}}(-\omega^{-2}) & S_{xx_{-1}}(-\omega^{-2}) & S_{xx_0}(-\omega^{-2}) & \cdots \\ & \vdots & \vdots & \vdots & \vdots & \vdots & \end{bmatrix} \tag{18}$$

$$\mathcal{S}_{uu}(\omega) = \begin{bmatrix} \vdots & \vdots & \vdots & \vdots & \vdots & \\ \cdots & S_{uu_0}(-\omega^2) & S_{uu_1}(-\omega^2) & S_{uu_2}(-\omega^2) & S_{uu_3}(-\omega^2) & S_{uu_4}(-\omega^2) & \cdots \\ \cdots & S_{uu_{-1}}(-\omega^1) & S_{uu_0}(-\omega^1) & S_{uu_1}(-\omega^1) & S_{uu_2}(-\omega^1) & S_{uu_3}(-\omega^2) & \cdots \\ \cdots & S_{uu_{-2}}(-\omega^0) & S_{uu_{-1}}(-\omega^0) & S_{uu_0}(-\omega^0) & S_{uu_1}(-\omega^0) & S_{uu_2}(-\omega^0) & \cdots \\ \cdots & S_{uu_{-3}}(-\omega^{-1}) & S_{uu_{-2}}(-\omega^{-1}) & S_{uu_{-1}}(-\omega^{-1}) & S_{uu_0}(-\omega^{-1}) & S_{uu_1}(-\omega^{-1}) & \cdots \\ \cdots & S_{uu_{-4}}(-\omega^{-2}) & S_{uu_{-3}}(-\omega^{-2}) & S_{uu_{-2}}(-\omega^{-2}) & S_{uu_{-1}}(-\omega^{-2}) & S_{uu_0}(-\omega^{-2}) & \cdots \\ & \vdots & \vdots & \vdots & \vdots & \vdots & \end{bmatrix} \tag{19}$$

When the T-periodic assumption of Equation 11 and the definitions of Equations 12 and 13 are applied to Equation 9, the following form is obtained for the two-dimensional power spectral densities S_{xx} and S_{uu} [5]:

$$S_{pp}(\omega_1,\omega_2) = \sum_{i=-\infty}^{\infty} S_{pp_i}(-\omega_1)\,\delta(\omega_1+\omega_2-i\omega_0) \tag{14}$$

Using Equation 14, the relation between the two-dimensional power spectral densities (Equation 10) is rewritten in terms of the (one-dimensional) harmonic PSDs S_{xx_i} and S_{uu_i}:

$$S_{xx_l}(-\omega) = \sum_{k,i=-\infty}^{\infty} H_i(\omega - i\omega_0)\,S_{uu_k}(-\omega+i\omega_0)\,H^T_{l-(i+k)}(-\omega+(i+k)\omega_0) \tag{15}$$

Equation 15, relating the harmonic PSDs of the input and output noise, is an extension to cyclostationary

Equation 16 expresses the relation between the output and input harmonic PSDs compactly using block matrices. Note from Equation 18 that the output harmonic PSDs evaluated at $\omega\,(=\omega^0)$ are given by the central block-row of $\mathcal{S}_{xx}$. The HPSDs of the self- and cross-powers of the p^{th} output x_p are available in the p^{th} row of this block. Denote the transpose of this row by $\mathcal{S}^T_{xx_{(\cdot,0)(\cdot,p)}}$; this is obtained by transposing Equation 16 and postmultiplying by a unit block-vector E_0 followed by the p^{th} unit vector e_p:

$$\mathcal{S}^T_{xx_{(\cdot,0)(\cdot,p)}}(\omega) = \overline{\mathcal{H}}(\omega)\,\mathcal{S}^T_{uu}(\omega)\,\mathcal{H}^T(\omega)\,E_0\,e_p \tag{20}$$

where

$$E_0 = \begin{bmatrix} \vdots \\ 0 \\ 0 \\ I_{n\times n} \\ 0 \\ 0 \\ \vdots \end{bmatrix} \leftarrow 0^{\text{th}} \text{ block}, \quad e_p = \begin{bmatrix} 0 \\ \vdots \\ \vdots \\ 1 \\ \vdots \\ 0 \end{bmatrix} \begin{matrix} \leftarrow 1^{\text{st}} \text{ entry} \\ \\ \\ \leftarrow p^{\text{th}} \text{ entry} \\ \\ \leftarrow n^{\text{th}} \text{ entry} \end{matrix} \quad (21)$$

$I_{n\times n}$ represents the $n \times n$ identity matrix. Note that $E_0\, e_p$ is a vector. Hence the computation of $\mathcal{S}^T_{xx_{(\cdot,0)(\cdot,p)}}(\omega)$ in Equation 20 can be performed by matrix-vector products with the block matrices $\mathcal{H}^T$, $\mathcal{S}^T_{uu}$ and $\overline{\mathcal{H}}$. Despite the fact that these matrices are, in general, dense, products with them can be performed efficiently, as discussed next in Sections 2.2 and 2.3.

2.2 Fast application of $\mathcal{H}^T$ and $\overline{\mathcal{H}}$ exploiting harmonic balance

To apply $\mathcal{H}^T$ and $\overline{\mathcal{H}}$ efficiently to a vector, it is necessary to represent $\mathcal{H}$ in terms of $C(t)$, $G(t)$ and A (refer Equation 2). Since $C(t)$ and $G(t)$ are T-periodic, they are expanded in Fourier series:

$$C(t) = \sum_{i=-\infty}^{\infty} C_i\, e^{ji\omega_0 t}, \quad G(t) = \sum_{i=-\infty}^{\infty} G_i\, e^{ji\omega_0 t} \quad (22)$$

The Fourier coefficients C_i and G_i will be referred to as the harmonics of $C(t)$ and $G(t)$ respectively. It can be shown [8] that $\mathcal{H}$ can be expressed in terms of these harmonics as:

$$\mathcal{H}(\omega) = J^{-1}(\omega)\,\mathcal{A}, \qquad J(\omega) = \mathcal{G} + j\Omega(\omega)\,\mathcal{C} \quad (23)$$

where

$$\mathcal{C} = \begin{bmatrix} \vdots & \vdots & \vdots & \vdots & \vdots & \\ \cdots & C_0 & C_{-1} & C_{-2} & C_{-3} & C_{-4} & \cdots \\ \cdots & C_1 & C_0 & C_{-1} & C_{-2} & C_{-3} & \cdots \\ \cdots & C_2 & C_1 & C_0 & C_{-1} & C_{-2} & \cdots \\ \cdots & C_3 & C_2 & C_1 & C_0 & C_{-1} & \cdots \\ \cdots & C_4 & C_3 & C_2 & C_1 & C_0 & \cdots \\ & \vdots & \vdots & \vdots & \vdots & \vdots & \end{bmatrix} \quad (24)$$

$$\mathcal{G} = \begin{bmatrix} \vdots & \vdots & \vdots & \vdots & \vdots & \\ \cdots & G_0 & G_{-1} & G_{-2} & G_{-3} & G_{-4} & \cdots \\ \cdots & G_1 & G_0 & G_{-1} & G_{-2} & G_{-3} & \cdots \\ \cdots & G_2 & G_1 & G_0 & G_{-1} & G_{-2} & \cdots \\ \cdots & G_3 & G_2 & G_1 & G_0 & G_{-1} & \cdots \\ \cdots & G_4 & G_3 & G_2 & G_1 & G_0 & \cdots \\ & \vdots & \vdots & \vdots & \vdots & \vdots & \end{bmatrix} \quad (25)$$

$$\Omega(\omega) = \begin{bmatrix} \ddots & & & & \\ & \omega^{-1}I & & & \\ & & \omega^{0}I & & \\ & & & \omega^{1}I & \\ & & & & \ddots \end{bmatrix} \quad (26)$$

$$\mathcal{A} = \begin{bmatrix} \ddots & & & & & & \\ & A & & & & & \\ & & A & & & & \\ & & & A & & & \\ & & & & A & & \\ & & & & & \ddots \end{bmatrix} \quad (27)$$

$J(\omega)$ is known as the *conversion matrix* [8] of the circuit; $J(0)$ is the Jacobian matrix of the harmonic balance equations at the circuit's steady state x^*.

For numerical computation, the infinite block matrices in Equations 17-19 and 24-27 are truncated to a finite number of blocks $N = 2M + 1$. M is the largest positive harmonic considered. For the purposes of the analysis, it is assumed that no significant harmonic PSD of degree greater than $M/2$ exists for the input noise $u(t)$ or the output noise $x(t)$. Since the energy content of the i^{th} harmonic is always a diminishing function of i in practical RF circuits, a value for M can always be found satisfying this assumption.

With this assumption, it can be shown that the Toeplitz block structure in the above matrices can be approximated by *circulant* block structure without loss of accuracy in the matrix-vector product. For example, $\mathcal{C}$ truncated to $N = 7$ blocks can be approximated by $\overset{\circ}{\mathcal{C}}$, given by:

$$\overset{\circ}{\mathcal{C}} = \begin{bmatrix} C_0 & C_{-1} & C_{-2} & C_{-3} & C_3 & C_2 & C_1 \\ C_1 & C_0 & C_{-1} & C_{-2} & C_{-3} & C_3 & C_2 \\ C_2 & C_1 & C_0 & C_{-1} & C_{-2} & C_{-3} & C_3 \\ C_3 & C_2 & C_1 & C_0 & C_{-1} & C_{-2} & C_{-3} \\ C_{-3} & C_3 & C_2 & C_1 & C_0 & C_{-1} & C_{-2} \\ C_{-2} & C_{-3} & C_3 & C_2 & C_1 & C_0 & C_{-1} \\ C_{-1} & C_{-2} & C_{-3} & C_3 & C_2 & C_1 & C_0 \end{bmatrix} \quad (28)$$

Note that the fourth, fifth and sixth sub- and super-diagonals of $\overset{\circ}{\mathcal{C}}$ differ from those of $\mathcal{C}$ truncated to 7 blocks. Matrix-vector products with $\overset{\circ}{\mathcal{C}}$ and the truncated $\mathcal{C}$, however, produce identical results upto the first harmonic location if the vector being multiplied contains no significant components in the second and third harmonic locations.

The utility of the circulant approximation is that it enables $\overset{\circ}{\mathcal{C}}$ and $\overset{\circ}{\mathcal{G}}$ to be decomposed into products of sparse block-diagonal matrices, permutations, and Fourier transform (DFT) matrices [4, 2, 3]. This enables matrix-vector products with $\overset{\circ}{\mathcal{C}}$ and $\overset{\circ}{\mathcal{G}}$ to be performed as a sequence of products with sparse block-diagonal matrices ($O(nN)$ operations), permutations (no cost), and Fourier transforms ($O(nN \log N)$ operations); hence the overall computation is $O(nN \log N)$. Further, since only the sparse block-diagonal matrices need to be stored, the memory requirement is $O(nN)$. Note that $\Omega(\omega)$ is a diagonal matrix with a-priori known entries ω^k, hence its application to a vector is $O(nN)$ in computational cost, with no memory required for its storage. The net effect of the circulant approximation, therefore, is that $J(\omega)$ can be applied to a vector in $O(nN \log N)$ computation and $O(nN)$ memory.

From Equation 23, it follows that to obtain the required matrix-vector product with $\mathcal{H}(\omega)$, matrix-vector products with $\mathcal{A}$ and $J^{-1}(\omega)$ are necessary. Since $\mathcal{A}$ is a sparse block-diagonal matrix with identical blocks A (the noise source incidence matrix), it can be applied in $O(nN)$ time and $O(n)$ memory. *Iterative linear solvers* [9, 10] can obtain the matrix-vector product with J^{-1} using only matrix-vector products with J. The use of iterative linear techniques, together with the decomposition of J allowing its application in $O(nN \log N)$ time, is the key to the fast harmonic balance algorithms of Rösch [2, 1, 3] and Melville et al [4]. With suitable preconditioning included in the iterative solution, the number of J-vector products required to compute a J^{-1}-vector product is small and approximately independent of the size of J. Hence the J^{-1}-vector product can be computed in approximately $O(nN \log N)$ time and $O(nN)$ memory, leading to the same computation and memory requirements for the desired product with $\mathcal{H}$.

From Section 2.1, products are required with $\mathcal{H}^T$ and $\overline{\mathcal{H}}$ for cyclostationary noise computation. Application of $\mathcal{H}^T$ is carried out using the same decomposition and iterative linear methods as for $\mathcal{H}$, but using transposes of the matrices involved. The product with $\overline{\mathcal{H}}$ is carried out using the relation $\overline{\mathcal{H}}\, z = \overline{\mathcal{H}\, \overline{z}}$.

2.3 Fast application of $\mathcal{S}_{uu}^T$

The principal sources of noise in circuits are thermal, shot and flicker $(1/f)$ noises from devices. When the linearized small-signal circuit (Equation 2) is time-invariant (i.e., the circuit is in DC steady state), these noise sources are stationary stochastic processes with known power spectral densities. Thermal and shot noises are white, with PSD values that are constant, independent of frequency; flicker noise PSDs exhibit a $\frac{1}{f}$ variation with frequency. The expressions for the power spectral densities of these noise sources (see, e.g., Van der Ziel [11]) typically involve some component of the DC solution; for example, the PSD of the shot noise current $u_D(t)$ across a diode's p-n junction is proportional to the DC current I_D through the junction, i.e.:

$$S_{u_D u_D}(\omega) = 2qI_D \tag{29}$$

where $S_{u_D u_D}(\omega)$ is the (stationary) PSD of the shot noise and q is the electronic charge.

From the viewpoint of second-order statistics, the diode's shot noise is equivalent to the hypothetical process generated by multiplying a white noise process $w(t)$ of PSD value $2q$ by a constant factor of $\sqrt{I_D}$:

$$u_D(t) = \sqrt{I_D}\, w(t), \qquad S_{ww}(\omega) = 2q \tag{30}$$

For this reason, shot noise is often said, in a loose sense, to be proportional to $\sqrt{I_D}$.

For circuits operating in DC steady state, expressions for PSDs of stationary noise generators are well established from theoretical considerations and/or through measurement. For circuits operating in time-varying steady state, unfortunately, there are as yet no stochastic models for the nonstationary noise generation process that are well established. Nevertheless, there is general consensus that for white processes like shot and thermal noise, the generated nonstationary or cyclostationary noise can be represented by the modulation of stationary white noise by deterministic time-varying parameters that depend on components of the large-signal steady state. For the diode shot noise example above, Equation 30 generalizes to:

$$u_D(t) = \sqrt{I_D(t)}\, w(t), \qquad S_{ww}(\omega) = 2q \tag{31}$$

where $I_D(t)$ is a time-varying waveform. Arguments supporting this deterministic modulation model are based on the short-term nature of the autocorrelations of thermal and shot noise; see, e.g., [12, 13, 14].

For noise with long-term correlations (notably flicker noise), there is a general belief that the above deterministic modulation of stationary noise model is inadequate [15]. The physical processes responsible for long-term correlations are expected to be modified by the time-varying large-signal waveforms. Unfortunately, neither theoretical analyses nor experimental data are available at this time, to the authors' knowledge, to validate the modulated stationary noise model or propose an alternative. Demir [13] uses the modulated stationary noise model for analyzing nonstationary flicker noise, and this model also appears to be commonly used among designers of RF circuits. The modulated stationary noise model is therefore reluctantly adopted in this work for all cyclostationary noise generators.

Under this noise generation model, the noise input $u(t)$ in Equation 2 can be expressed as:

$$u(t) = M(t)\, u_s(t) \tag{32}$$

where $u_s(t)$ is an m-dimensional vector of stationary noise sources and $M(t)$ is an $m \times m$ diagonal matrix of T-periodic deterministic modulations.

Equation 16 can be used to analyze the relation between statistics of $u(t)$ and $u_s(t)$ by recognizing that Equation 32 represents an LTV system with input $u_s(t)$ and output $u(t)$. The time-varying impulse response of the LTV system is:

$$h(t_2, t_1) = \delta(t_2 - t_1)\, M(t_2) = \sum_{i=-\infty}^{\infty} M_i\, \delta(t_2 - t_1)\, e^{j i \omega_0 t_2} \tag{33}$$

M_i denote the Fourier coefficients of the periodic modulation $M(t)$. The harmonic transfer functions $H_i(\omega)$ are independent of ω and simply equal to M_i. Equation 16 applied to this LTV system results in the following block-matrix relation between the harmonic PSDs of $u(t)$ and $u_s(t)$:

$$\mathcal{S}_{uu}(\omega) = \mathcal{M}\, \mathcal{S}_{u_s u_s}(\omega)\, \mathcal{M}^* \tag{34}$$

$\mathcal{S}_{u_s u_s}(\omega)$ represents the block Toeplitz matrix of the harmonic PSDs of the stationary noise sources. Since the sources are stationary, all their harmonic PSDs are zero except for the stationary PSD $S_{u_s u_{s_0}}(\omega)$; hence

$\mathcal{S}_{u_s u_s}(\omega)$ is block diagonal with diagonal entries $[\cdots, S_{u_s u_{s0}}(-\omega^2), S_{u_s u_{s0}}(-\omega^1), S_{u_s u_{s0}}(-\omega^0), S_{u_s u_{s0}}(-\omega^{-1}), S_{u_s u_{s0}}(-\omega^{-2}), \cdots]$. $\mathcal{M}$ in Equation 34 is block Toeplitz with M_i in the diagonals:

$$\mathcal{M} = \begin{bmatrix} & \vdots & \vdots & \vdots & \vdots & \vdots & \\ \cdots & M_0 & M_1 & M_2 & M_3 & M_4 & \cdots \\ \cdots & M_{-1} & M_0 & M_1 & M_2 & M_3 & \cdots \\ \cdots & M_{-2} & M_{-1} & M_0 & M_1 & M_2 & \cdots \\ \cdots & M_{-3} & M_{-2} & M_{-1} & M_0 & M_1 & \cdots \\ \cdots & M_{-4} & M_{-3} & M_{-2} & M_{-1} & M_0 & \cdots \\ & \vdots & \vdots & \vdots & \vdots & \vdots & \end{bmatrix} \quad (35)$$

Using Equation 34, the product of $\mathcal{S}_{uu}$ with a vector can be performed through matrix-vector products with the matrices $\mathcal{M}$, $\mathcal{M}^*$ and $\mathcal{S}_{u_s u_{s0}}$. Products with the block-Toeplitz matrices $\mathcal{M}$ and $\mathcal{M}^*$ can be performed in $O(mN \log N)$ time and $O(mN)$ memory, approximating $\mathcal{M}$ by a block-circulant matrix and applying the same decomposition as for $\mathcal{G}$ in Section 2.2. Application of the block-diagonal matrix $\mathcal{S}_{u_s u_s}(\omega)$ is equivalent to N matrix vector products with $S_{u_s u_{s0}}(\cdot)$. If the device noise generators are uncorrelated, $S_{u_s u_{s0}}(\cdot)$ is diagonal; if correlations exist, they are usually between small groups of noise generators, hence $S_{u_s u_{s0}}(\cdot)$ is sparse. In either case, each product with $S_{u_s u_{s0}}(\cdot)$ is $O(m)$ in computation with no storage required. Hence matrix-vector products with $\mathcal{S}_{u_s u_{s0}}$ $O(Nm)$ time and $O(1)$ memory. The overall matrix-vector product with $\mathcal{S}_{uu}$ can therefore be performed in $O(mN \log N)$ time and $O(mN)$ memory.

It should be noted that the noise modulation $M(t)$ can be absorbed into the circuit equations (Equation 1). The noise inputs $u(t)$ to the circuit can then be assumed to be stationary without loss of generality. This procedure, however, increases the size of the harmonic balance system for obtaining the steady state x^*. To avoid this and to separate the implementation of the noise algorithm from the harmonic balance steady state algorithm, the formulation of this section is preferred.

3 Bandpass filtering of cyclostationary noise

Ström and Signell [5] have shown that low-pass filtering of cyclostationary noise results in stationary noise if the bandwidth of the low-pass filter is less than half the frequency of cyclostationarity ω_0. This result has been used by Hull and Meyer [16] to simplify their analysis. In this section, the effect of LTI band-pass filtering on cyclostationary noise is considered. It is shown that if cyclostationary noise is passed through a one-sided (i.e., single-sideband) band-pass filter of bandwidth less than $\frac{\omega_0}{2}$, the output noise is stationary. This result is obtained using a simple visualization of the propagation of harmonic PSDs.

Denote the input noise to a band-pass filter by $n(t)$ and the output noise by $x(t)$. Assume that the input $n(t)$ is cyclostationary with period $T = \frac{2\pi}{\omega_0}$. Denote the transfer function of the band-pass filter by $H(\omega)$. The relationship between the harmonic PSDs of $n(t)$ and

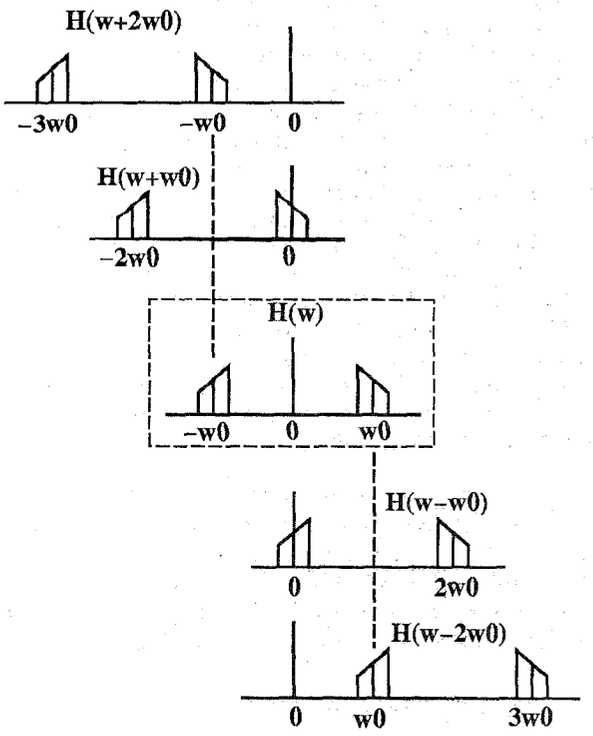

Figure 1: $H(\omega)$ overlaid with $H(\omega + i\omega_0)$ for i= 2, 1, -1 and -2

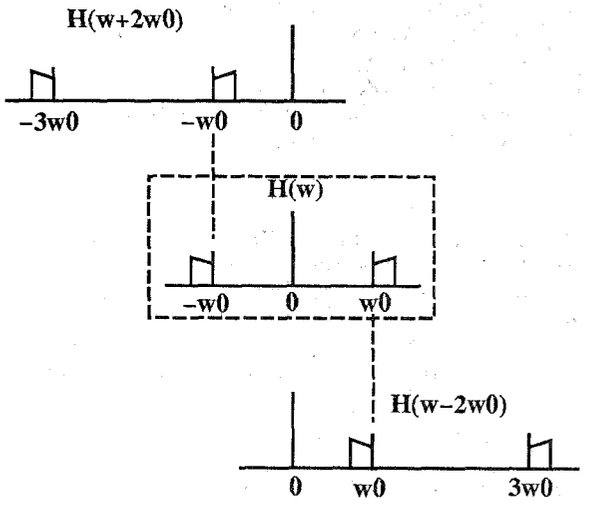

Figure 2: One-sided $H(\omega)$ overlaid with $H(\omega + i\omega_0)$ for i= 2 and -2

$x(t)$, derived from Equation 20 by using the fact that $\mathcal{H}$ is block diagonal for a LTI network, is:

$$S_{xx_i}(\omega) = H(-\omega)\, S_{nn_i}(\omega)\, H^T(\omega + i\omega_0) \qquad (36)$$

Note that the i^{th} harmonic PSD of the output is determined completely by the corresponding harmonic PSD of the input, shaped by the product of the filter function $H(\omega)$ with a shifted version of itself $H^T(\omega + i\omega_0)$. For the scalar input-output case under consideration, the relation simplifies to:

$$S_{xx_i}(\omega) = H(-\omega)\, H(\omega + i\omega_0)\; S_{nn_i}(\omega) \qquad (37)$$

Since the magnitude of $H(\omega)$ for a real filter is symmetric about zero, $H(-\omega)$ has the same magnitude characteristic as $H(\omega)$. By overlaying the magnitudes of $H(\omega)$ and $H(\omega + i\omega_0)$ for different values of i (illustrated in Figure 1), it can be seen that the product $H(-\omega)\, H(\omega + i\omega_0)$ is nonzero only for i=0, 2, and -2 if the bandwidth of $H(\omega)$ is less than $\frac{\omega_0}{2}$. For all other values of i, there is no frequency at which $H(-\omega)$ and $H(\omega + i\omega_0)$ are both nonzero, hence their product is identically zero.

This immediately implies the following result:

Result 1: *Bandpass filtering with bandwidth less than $\frac{\omega_0}{2}$ eliminates all harmonic PSDs except the stationary and second harmonic PSDs.*

Moreover, if the band-pass filter is one-sided with respect to ω_0, then the product $H(\omega)\, H(\omega + i\omega_0)$ is identically zero also for i=2 and -2, as illustrated in Figure 2. In this case, the bandwidth of the filter can be greater than $\frac{\omega_0}{2}$ but should be less than ω_0. The only nonzero PSD of the output is then the stationary PSD. This implies

Result 2: *One-sided (or single-sideband) bandpass filtering (with bandwidth less than ω_0) of cyclostationary noise results in stationary output noise.*

4 Experimental Results

The fast cyclostationary noise algorithm of Section 2 has been prototyped in a Bell Labs internal simulator. Two circuit examples are presented in this section.

4.1 Mixer and bandpass filter

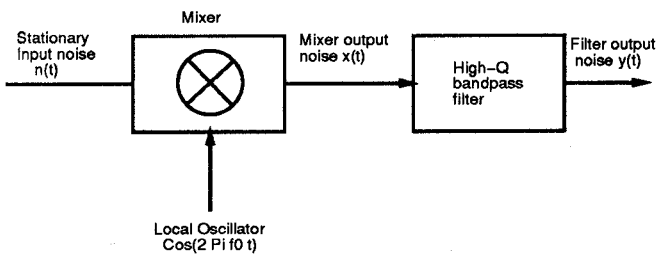

Figure 3: Mixer and bandpass filter

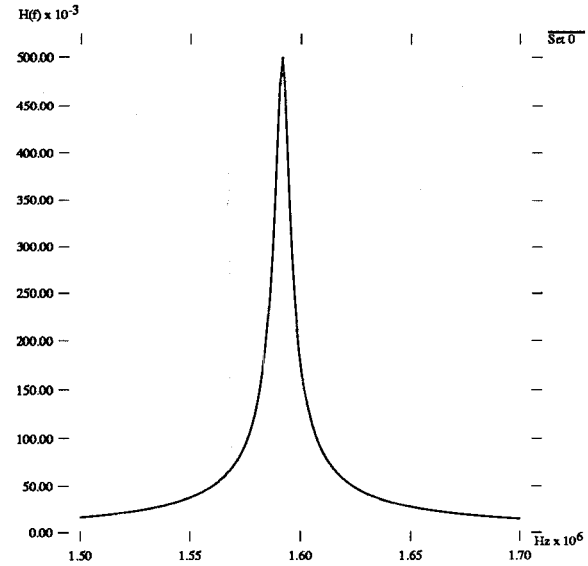

Figure 4: Bandpass filter characteristic

Motivated by the result of Section 3, a mixer and bandpass filter circuit (Figure 3) is analyzed for cyclostationary noise propagation. The mixer is an ideal multiplier that modulates the incoming stationary noise with a deterministic LO oscillator signal $\cos(2\pi f_0 t)$. The filter has a high-Q bandpass characteristic (illustrated in Figure 4) with a center frequency of approximately 1.592 Mhz and a bandwidth of about 50 KHz. The stationary input noise is bandlimited with double-sided bandwidth of about 200 KHz.

Two simulations are carried out, with f_0 set to 1.592 Mhz and 1.5 Mhz respectively. In the first situation, the bandpass filter is centered at the LO frequency; in the second, the filter characteristic is offset to the right of the LO frequency, strongly attenuating the lower sideband with respect to f_0 while passing the upper sideband. Harmonic PSDs at all nodes in the circuit were computed over frequencies from 1Mhz to 2Mhz.

Using the results of Section 2.1, it can be shown that only the stationary and second harmonic PSDs of the mixer output $x(t)$ are nonzero, related to the PSD of the stationary input by:

$$S_{xx_0}(\omega) = \frac{S_{nn_0}(\omega - \omega_0) + S_{nn_0}(\omega - \omega_0)}{4}$$

$$S_{xx_{-2}}(\omega) = \frac{S_{nn_0}(\omega - \omega_0)}{4}, \quad S_{xx_2}(\omega) = \overline{S_{xx_{-2}}(-\omega)}$$

The stationary and second harmonic PSDs of the filter output $y(t)$ for f_0=1.592 Mhz (double sideband filtering) are shown in Figures 5 and 6. It can be seen that both PSDs have the same magnitude, hence there is a large cyclostationary component in the noise. The same PSDs for the f_0=1.5 Mhz case (single sideband filtering) are shown in Figures 7 and 8. The second harmonic PSD can be seen to be about two orders of magnitude smaller than the stationary PSD. Hence the

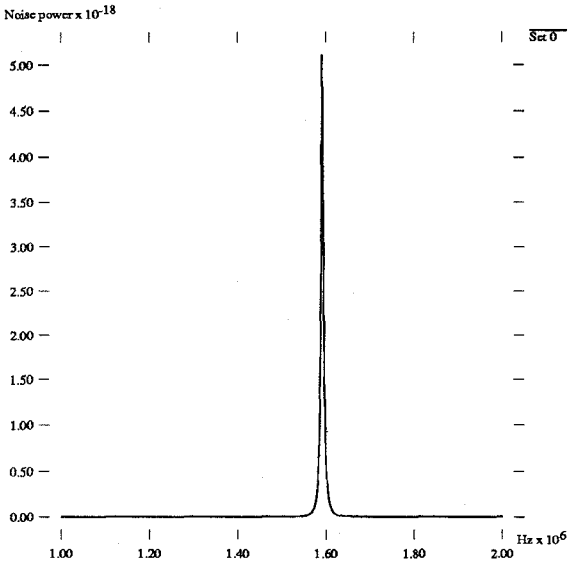

Figure 5: $S_{yy_0}(f)$ with f_0=1.592 Mhz (double-sideband filtering)

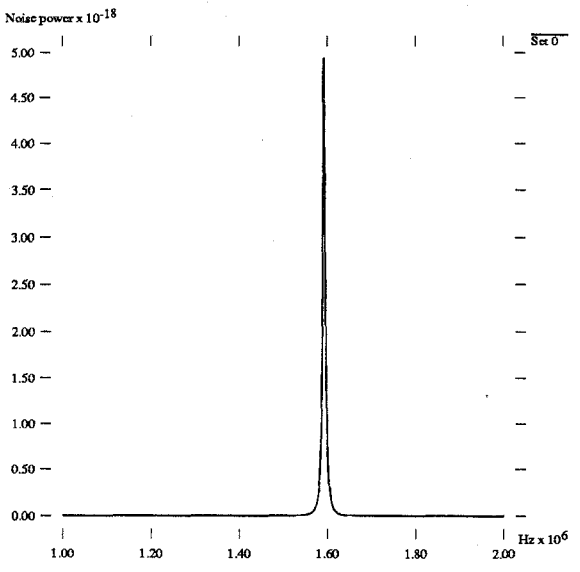

Figure 6: $S_{yy_{-2}}(f)$ with f_0=1.592 Mhz (double-sideband filtering)

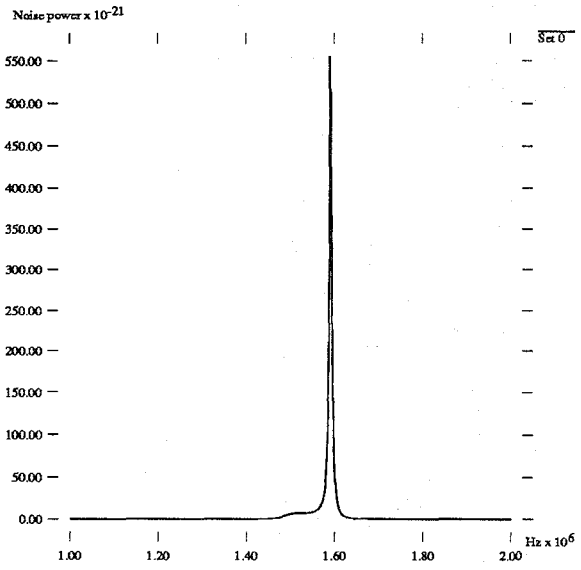

Figure 7: $S_{yy_0}(f)$ with f_0=1.5 Mhz (single-sideband filtering)

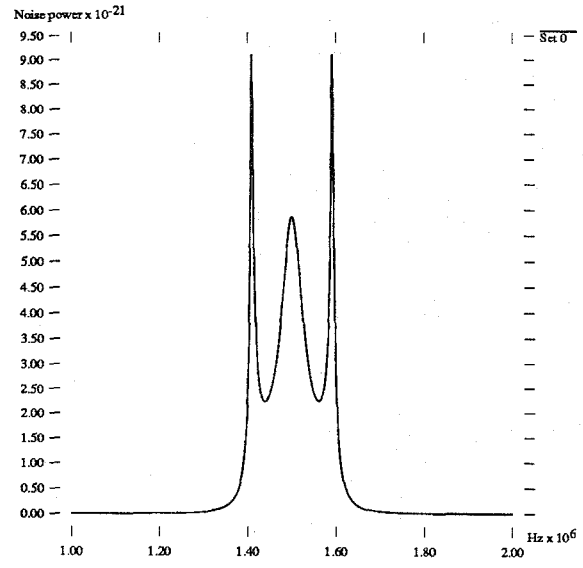

Figure 8: $S_{yy_{-2}}(f)$ with f_0=1.5 Mhz (single-sideband filtering)

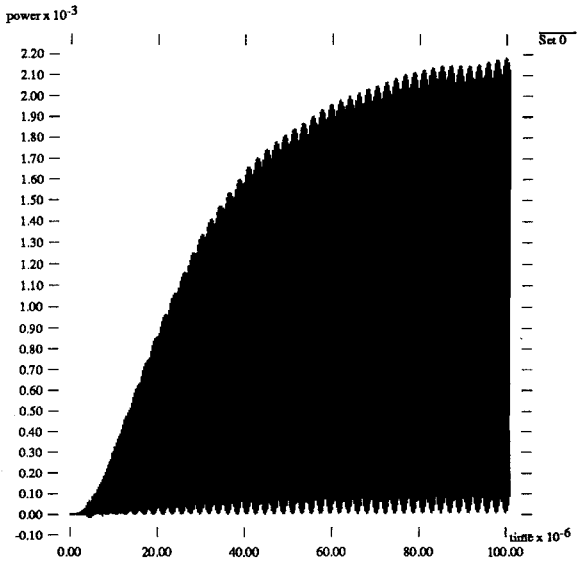

Figure 9: Time-varying filtered noise power from Monte-Carlo: f_0=1.592 Mhz (double-sideband)

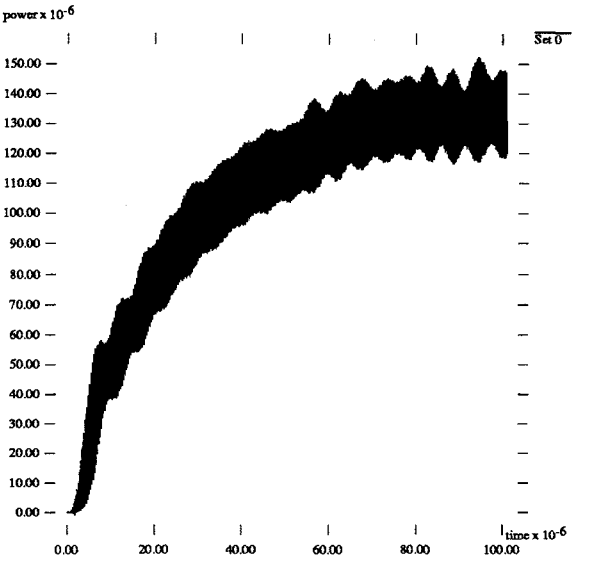

Figure 10: Time-varying filtered noise power from Monte-Carlo: f_0=1.5 Mhz (single-sideband)

filtered noise is virtually stationary, as predicted in Section 3. The second harmonic PSD is not identically zero because the non-ideal single-sideband filter does not perfectly eliminate the lower sideband.

The above results were also verified by simulations using the Monte-Carlo method. The nonlinear differential equations of the circuit in Figure 3 were solved numerically with 60,000 samples of the input noise $n(t)$ [17]. The input noise PSD was normalized to 1 to avoid corruption of the results by numerical noise generated during differential equation solution. The 60,000 samples of the mixed and filtered noise $y(t)$ were squared and averaged, on a per-timepoint basis, to obtain the noise power at the output as a function of time. The variation of noise power with time is shown in Figures 9 and 10 for the double-sideband and single-sideband cases. When analyzed in the time domain, the circuit requires some time to reach large-signal steady state, hence the steady state noise power is approached toward t = 100ms; in contrast, harmonic balance calculates this steady state directly. The cyclostationarity of the noise in the double-sideband case can be seen from the variation of the power between zero and its maximum value of about 0.0022. In the single-sideband case, the power approaches a steady value of about 130×10^{-6}, with a cyclostationary variation of about 10%. Accounting for the normalization of the input PSD, these values are in excellent agreement with the total integrated noise of $S_{yy_0}(f)$ and $S_{yy_{-2}}(f)$ (Figures 7 and 8); Monte-Carlo simulation results are within 2% of the results produced by the new algorithm.

4.2 I-Q mixer/buffer circuit

An integrated RF design, consisting of mixers and buffers in the in-phase and quadrature signal paths of a receiver, was simulated for cyclostationary noise. The circuit consisted of more than 50 bipolar devices and about 360 nodes. Previous algorithms for nonlinear noise are unable to analyze circuits of this size on account of their large computation and memory requirements.

The circuit was simulated on one processor of a high-end SGI workstation[1]. Noise was analyzed at 20 frequency points, swept from 100kHz to 2Mhz. 22 harmonics were used to account for nonlinearities. The simulation completed in 1 hour and 29 minutes of CPU time and used 50MB of memory. The stationary component of the noise at one of the nodes of the circuit is shown in Figure 11.

5 Conclusion

A efficient frequency-domain algorithm has been presented for computing noise in nonlinear circuits. The method uses harmonic PSDs in its noise formulation. A block-structured matrix equation for the output noise statistics is the central result enabling the fast algorithm.

The new formulation was used to prove that one-sided bandpass filtering of cyclostationary noise produces stationary noise. This extends a previously known result for lowpass filtering.

Results from the new algorithm were shown to match Monte-Carlo simulation outputs to an accuracy of 2%.

[1] An IRIX64 machine with 4 processors and 1.5GB of memory, running Irix6.2.

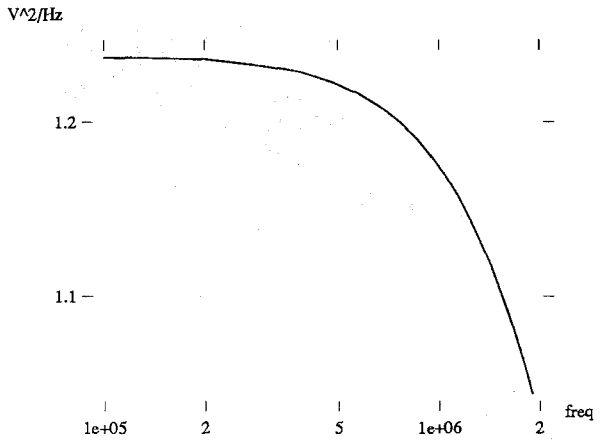

Figure 11: Stationary PSD for the I-Q mixer/buffer circuit

A large industrial RF circuit, containing more than 300 nodes, was simulated for noise in less than two hours on a fast workstation.

Acknowledgments

We would like to thank Mihai Banu, Laszlo Toth, Alex Dec, Ken Suyama, Venu Gopinathan and Bob Meyer for useful discussions regarding the RF noise problem. The efficient harmonic balance algorithm used in this work was developed with our colleagues Bob Melville and David Long.

References

[1] M. Rösch and K.J. Antreich. Schnell stationäre Simulation nichtlinearer Schaltungen im Frequenzbereich. *AEÜ*, 46(3):168–176, 1992.

[2] Markus Rösch. *Schnell Simulation des stationären Verhaltens nichtlinearer Schaltungen.* PhD thesis, Technischen Universität München, 1992.

[3] H.G. Brachtendorf, G. Welsch, R. Laur, and A. Bunse-Gerstner. Numerical steady state analysis of electronic ciercuits driven by multi-tone signals. *Electrical Engineering (Springer-Verlag)*, 79:103–112, 1996.

[4] R.C. Melville, P. Feldmann, and J. Roychowdhury. Efficient multi-tone distortion analysis of analog integrated circuits. In *Proc. IEEE CICC*, May 1995.

[5] T. Ström and S. Signell. Analysis of Periodically Switched Linear Circuits. *IEEE Trans. Ckts. Syst.*, CAS-24(10):531–541, Oct 1977.

[6] A. Papoulis. *Probability, Random Variables and Stochastic Processes.* McGraw-Hill Series in System Science. McGraw-Hill, New York, 1965.

[7] W. Gardner. *Introduction to Random Processes.* McGraw-Hill, New York, 1986.

[8] S.A. Haas. *Nonlinear Microwave Circuits.* Artech House, Norwood, MA, 1988.

[9] R. Freund, G.H. Golub, and N.M. Nachtigal. Iterative solution of linear systems. *Acta Numerica*, pages 57–100, 1991.

[10] Y. Saad. *Iterative methods for sparse linear systems.* PWS, Boston, 1996.

[11] A. Van der Ziel. *Noise in solid state devices and circuits.* Wiley, New York, 1986.

[12] M. Okumura, H. Tanimoto, T. Itakura, and T. Sugawara. Numerical Noise Analysis for Nonlinear Circuits with a Periodic Large Signal Excitation Including Cyclostationary Noise Sources. *IEEE Trans. Ckts. Syst. - I: Fund. Th. Appl.*, 40(9):581–590, September 1993.

[13] A. Demir. Time Domain Non Monte Carlo Noise Simulation For Nonlinear Dynamic Circuits with Arbitrary Excitations. Technical Report Memorandum no. UCB/ERL M94/39, EECS Dept., Univ. Calif. Berkeley, 1994.

[14] V. Rizzoli and A. Neri. State of the Art and Present Trends in Nonlinear Microwave CAD Techniques. *IEEE Trans. MTT*, 36(2):343–365, February 1988.

[15] M. Banu, V. Gopinathan, R. Meyer, and Y. Tsividis. Personal communications, 1996.

[16] C. Hull and R.G. Meyer. A Systematic Approach to the Analysis of Noise in Mixers. *IEEE Trans. Ckts. Syst. - I: Fund. Th. Appl.*, 40(12):909–919, December 1993.

[17] J. Roychowdhury and P. Feldmann. Generating Stationary Noise For Circuit Noise Simulation, July 1996. In preparation.